

Finite Element Analysis (FEA) Report

Job #1

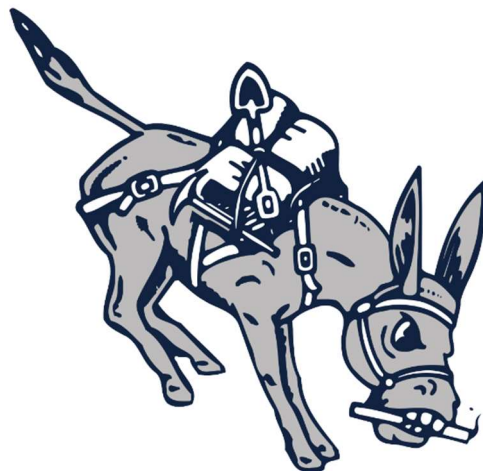
Double Wishbone Analysis

May 30, 2025



Rev.0

Jackson McCool



Executive Summary

Problem Statement & Summary

The objective was to analyze a wishbone suspension system to determine functionality under different shock configurations and perform an optimization study on the lower suspension arm. The goal of the optimization study is to minimize the mass while maintaining the factor of safety above 3.5. Active use conditions are modeled, the forces applied from the vehicle are assumed to be fixed forces applied to the system.

Analysis Methods Used

The suspension system was analyzed using Finite Element Analysis (FEA) within the Solidworks simulation software (SWS). The results were validated by hand calculations. The assembly was fixed with hinge connections where the system would connect to the vehicle frame and two directional forces were applied where the assembly would connect to the wheel and brake assemblies. The shock was modeled as a spring to simulate different shock conditions. The lower suspension arm was simulated in isolation with reaction forces determined with statics principles.

Results

The system was found to act identically in terms of stress when the shock conditions were altered. The stress in the lower suspension arm acted the same in isolation and an optimal variation was found with 19.2% weight savings with a factor of safety of 3.7. The FEA was validated with hand calculations determined to be within an acceptable range of error based off assumptions made, 12.3%. It is recommended that experimental testing take place to verify the result of this study as both the hand calculations and the SWS analysis require imperfect assumptions. Figure 1 shows the Von Mises stress for both the base assembly and optimized lower suspension arm.

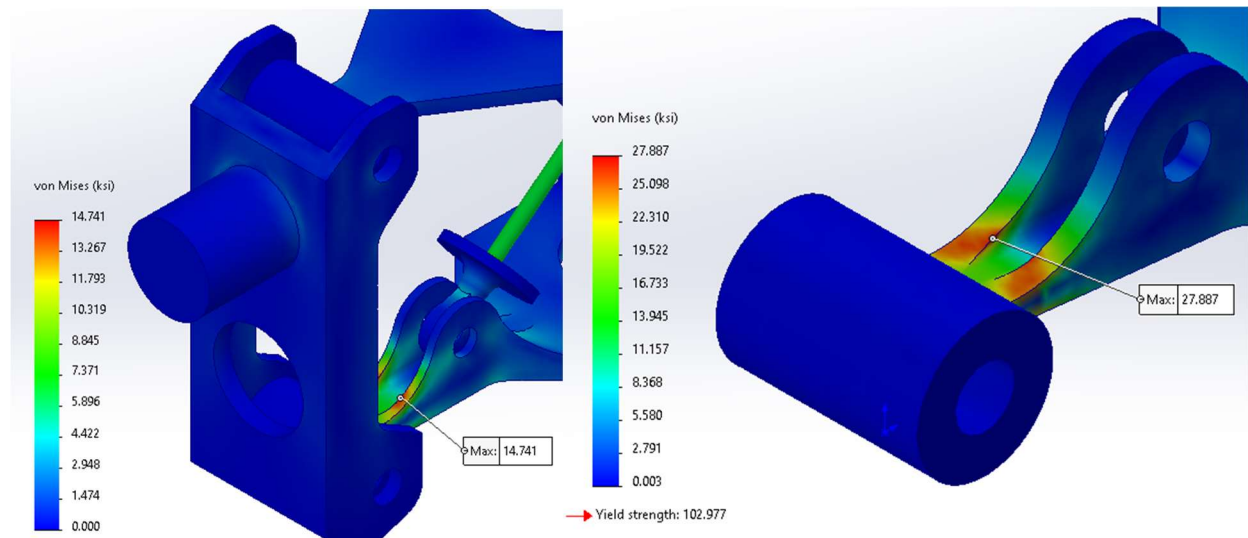


Figure 1 - Max Von Mises, initial assembly & optimized lower suspension arm

Background & Introduction

Figure 1 shows the proposed “double wishbone” suspension assembly. The assembly uses pin attachments at points D, C, and B and attaches to the full vehicle assembly via hinges at points G and E, figure 2.

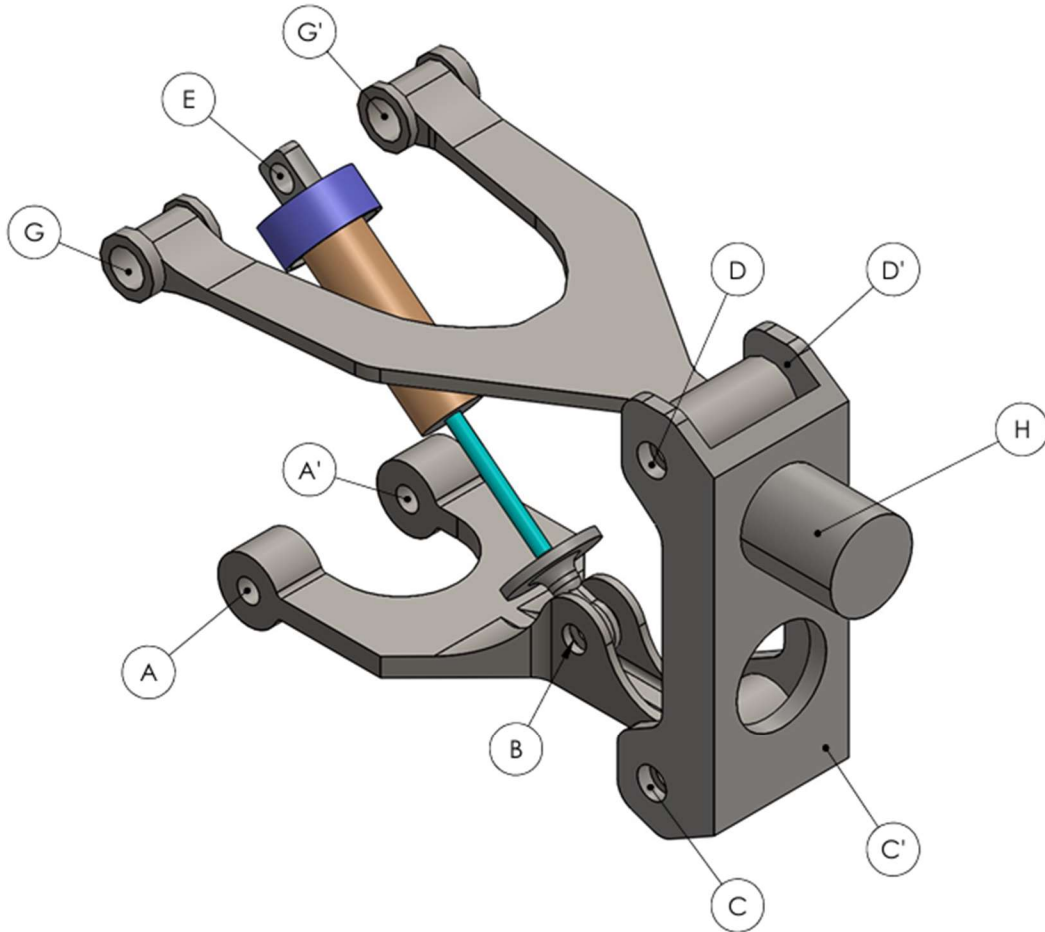


Figure 2 - Full Assembly Iso View

The goal of this analysis was to determine stresses on the assembly under load. To simulate this a computational model will be made with external force to simulate this. Different spring stiffnesses along the plunger will also be simulated.

An optimization study will also be done while analyzing only the lower suspension arm in isolation to optimize mass while keeping the factor of safety above 3.5.

System Configuration

The system being analyzed is made up of three stiff sections connected via pins with the shock system acting as a two-force member. The shock acts through the same hinge in the top left and moves through a pin connection with the lower suspension arm. The major dimension can be seen in figure 3.

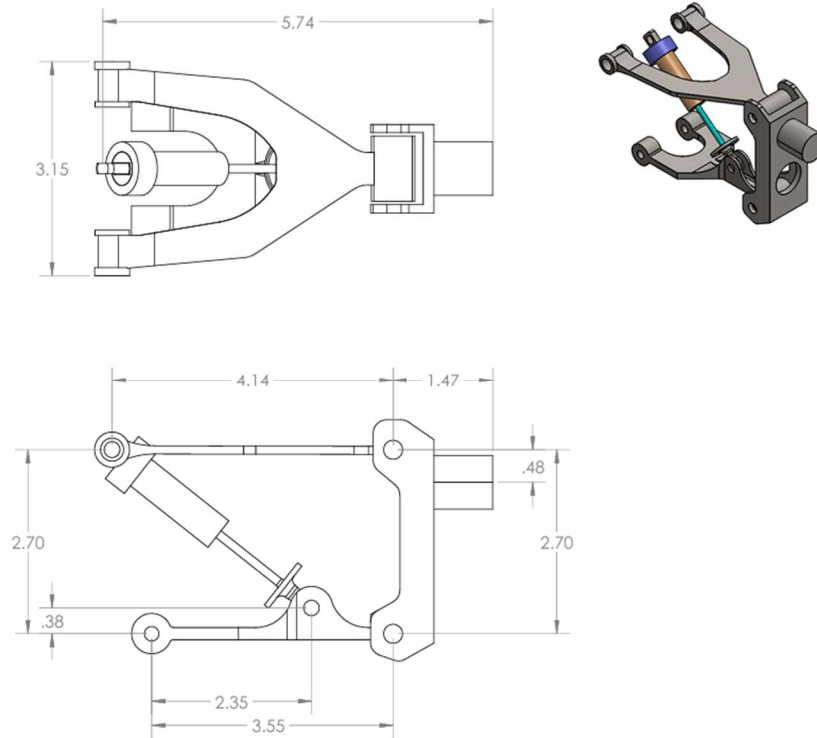


Figure 3 - Major Assembly Dimensions

The major dimensions of the lower suspension arm can be seen in figure 4, the dimensions labeled GAP and THICKNESS will be used in the optimization study.

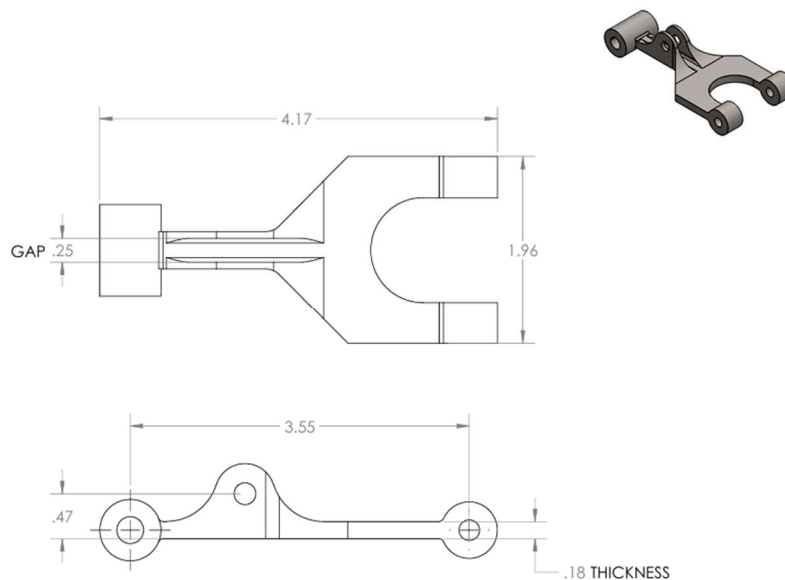
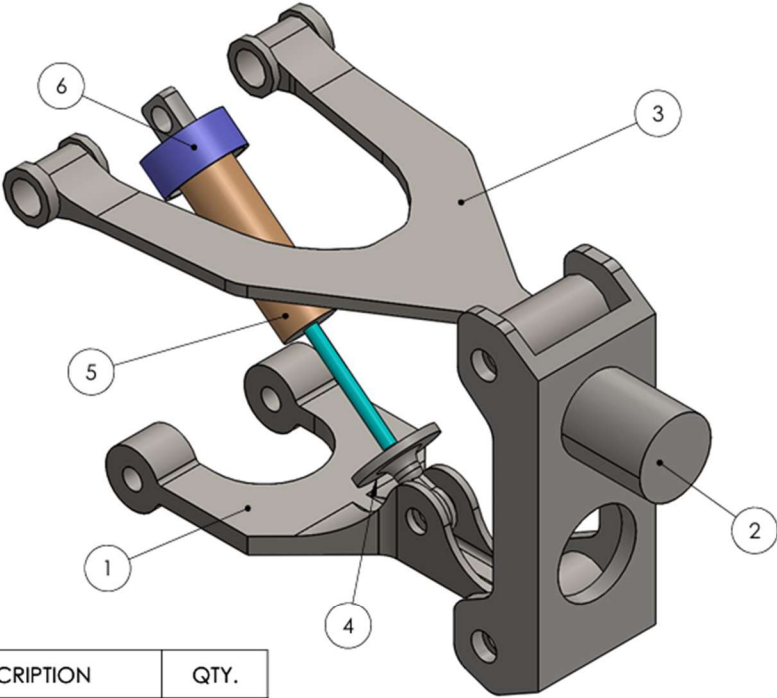


Figure 4 - Lower Suspension Arm Major Dimensions

System Properties

This assembly is made of parts of differing materials, figure 5. Relevant material properties for each material can be found in appendix A.



ITEM NO.	PART NUMBER	DESCRIPTION	QTY.
1	lower arm v4	AISI 4340 Steel	1
2	Knuckle	Cast Carbon Steel	1
3	upper arm	AISI 4340 Steel	1
4	shock plunger	Cast Carbon Steel	1
5	shock tube	Cast Carbon Steel	1
6	front shock clamp	Cast Carbon Steel	1

Figure 5 - Individual Part Materials

System Conditions

The full assembly model is used in an FEA model with the following loading and fixtures, refer to figure 1 for point labels. Hinge supports are used on points G and E. Two forces, F_x and F_y , are applied at point H. Points B, C, and D are modeled using pins. Figure 6.

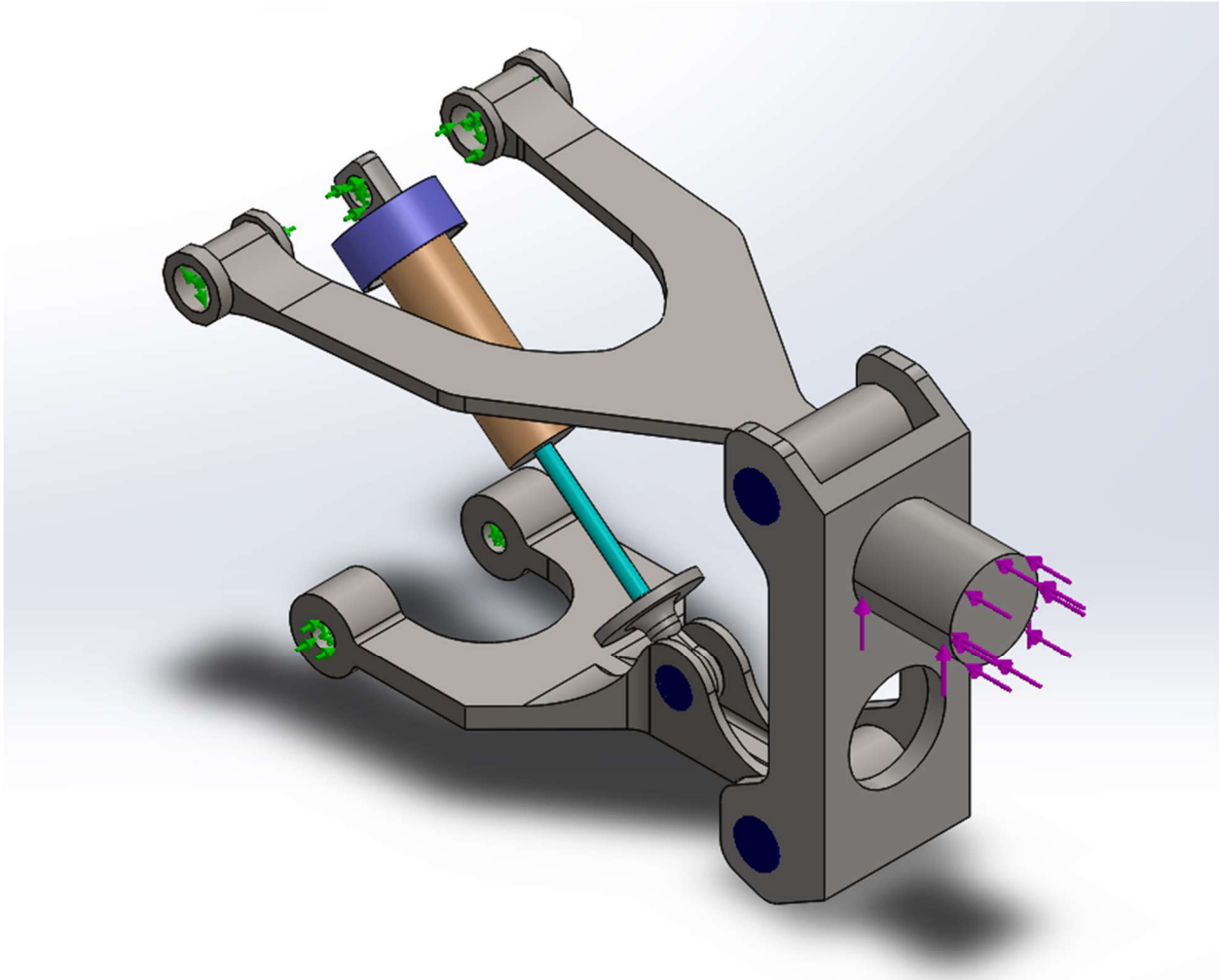


Figure 6 - Full Assembly locked piston configuration

This model was simulated with three different variations of the shock, a perfectly stiff shock, where the assembly parts were modeled as bonded. Then two spring connections were modeled, one at 450 lbs and the other at 900 lbs, figures 7 and 8.

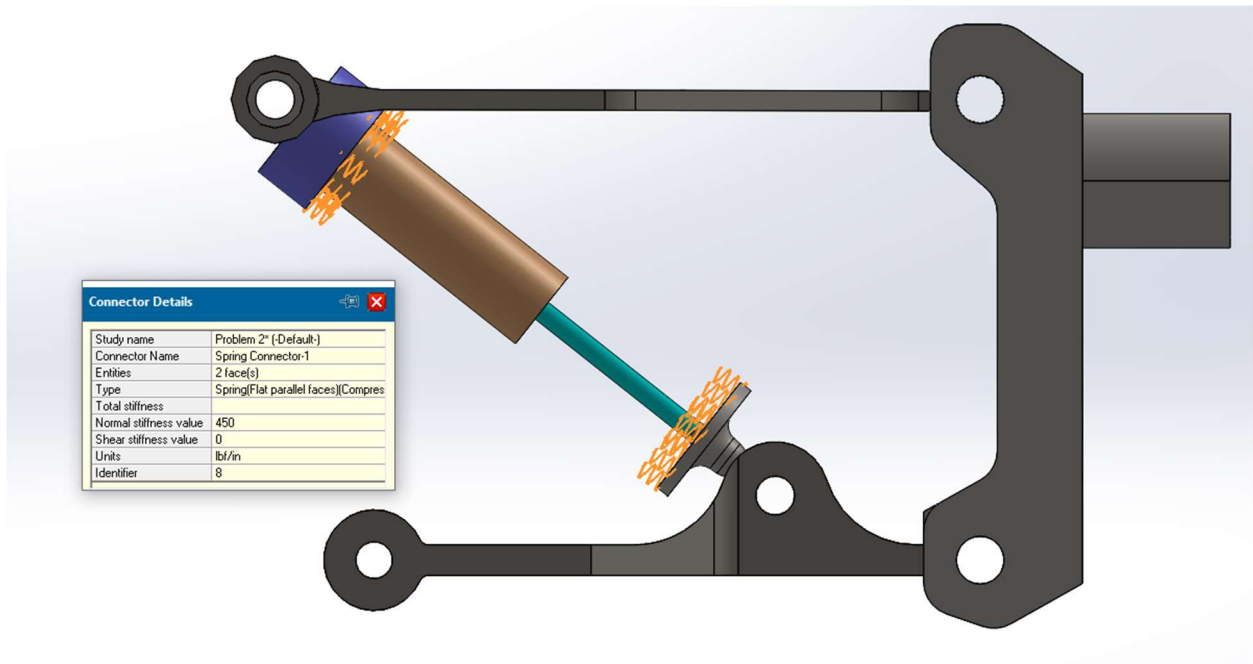


Figure 7 - 450 lbs spring configuration

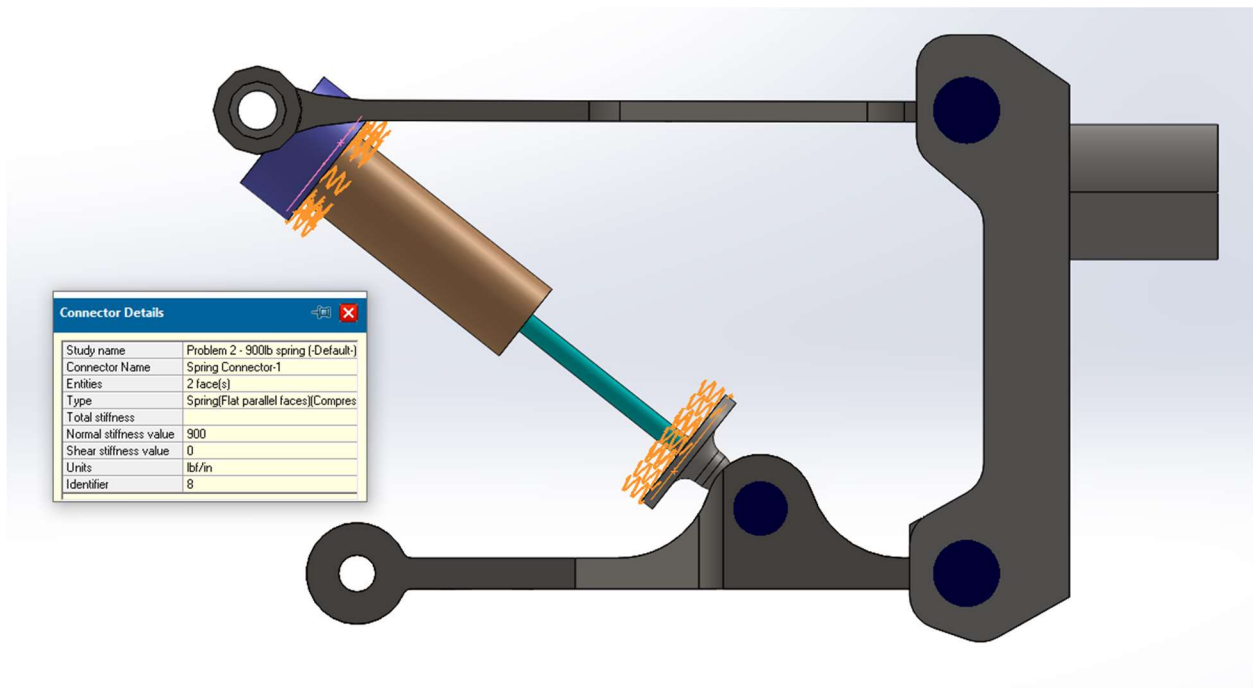


Figure 8 - 900 lbs spring configuration

The isolated lower suspension model was modeled with forces placed at points B and C with a hinge fixture at D as seen in figure 9.

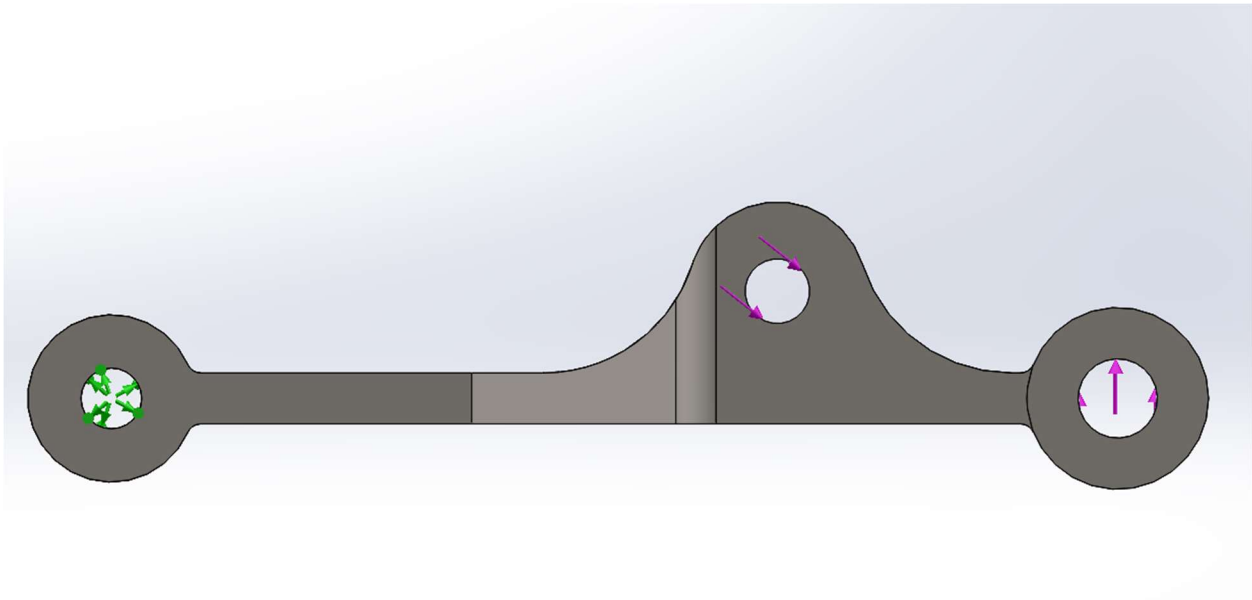


Figure 9 - Lower suspension arm isolated configuration

The forces were applied on split lines to mimic the reaction forces, the statics can be viewed in appendix B, the angle of the split lines can be seen in figure 10.

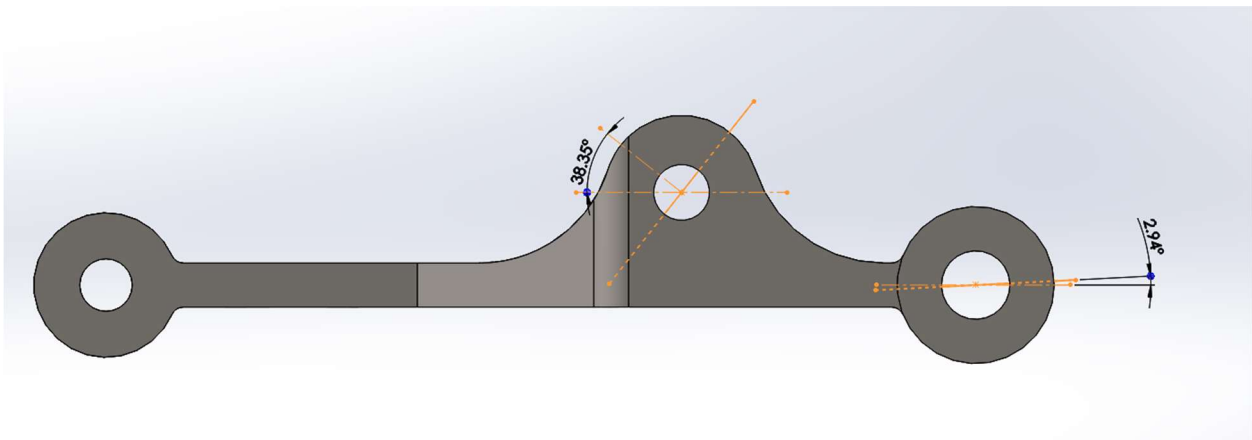


Figure 10 - Split line angles

System Discretization

A default mesh of 0.155 in was used for the model as there were no areas of large stress intensity. A mesh convergence study was also conducted. Ensuring the mesh converged within 5% of the previous density to ensure accurate results without overextending resources during the simulation process. The calculated percent difference was 3.45% see figure 11 for data.

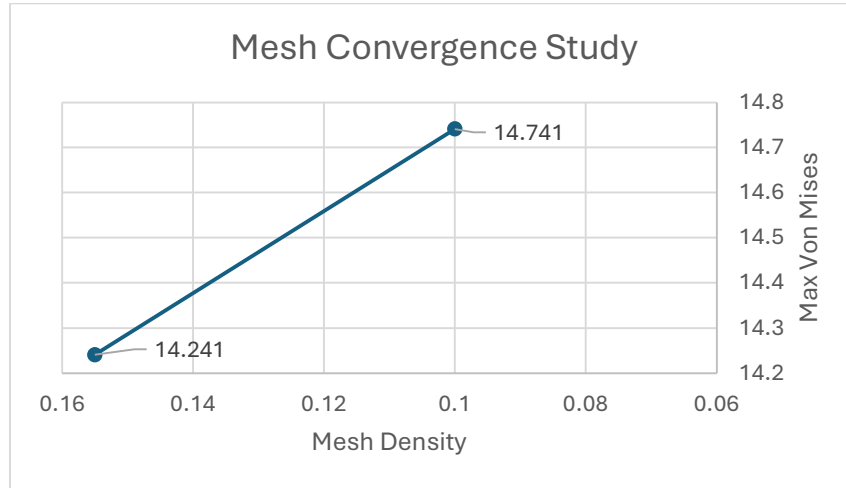


Figure 11 - Mesh Convergence Study

Mesh control around the inner shock tube and shock plunger was used to ensure proper modeling of the contact between the parts. To ensure this mesh was sufficient the deflection of the model was simulated to ensure proper interaction. Figure 12 shows the mesh control.

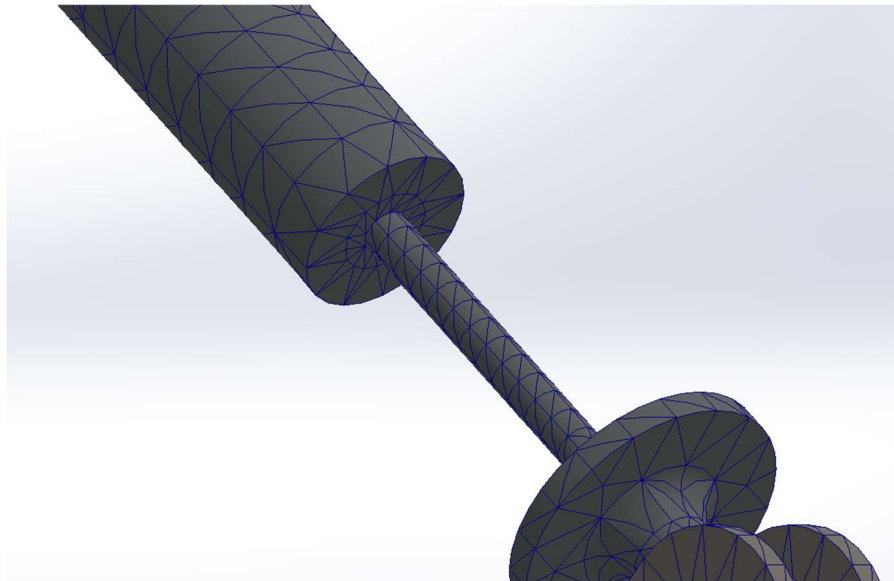


Figure 12 - Mesh Control around contact interaction

Verification & Validation

Hand calculations were performed to verify the results of the FEA model. Statics and solid mechanics principles were used to find reaction forces along the lower suspension arm and find the max stress along the top edge to verify the location and magnitudes found in the FEA model, found to be 10.65 ksi, appendix C.

These calculations are simplified and do not take into account the deflection of the assembly or the interactions between members. This means there may be stresses not accounted for within the hand calculations. Experimental results are necessary to fully validate the FEA model.

There are multiple experimental setups that could be used to verify the model. A whole system experiment would require a jig that could hold points X and Y so that they are fixed in translation but allowed to rotate as hinges. A calibrated hydraulic piston, like those found in hydraulic presses, should be angled at X degrees and apply a force of 85 lbf at point H. This experiment could verify the results of the different shock variations.

It would also be possible to experiment on the lower suspension arm in isolation. This would require a similar hinge fixture at point X while multiple pistons would need to be placed to simulate the reaction forces within the part. This experiment could test different variations of the lower suspension arm to validate the design optimization.

Results

The maximum stress in the assembly was found to be on the lower suspension arm. The maximum Von Mises stress remained around 14 ksi in all configurations. There was nearly no stress in other parts of the assembly with the only notable exception being the locked shock where there was stress around 7.5 ksi throughout the shock plunger, figures 13 and Appendix D.

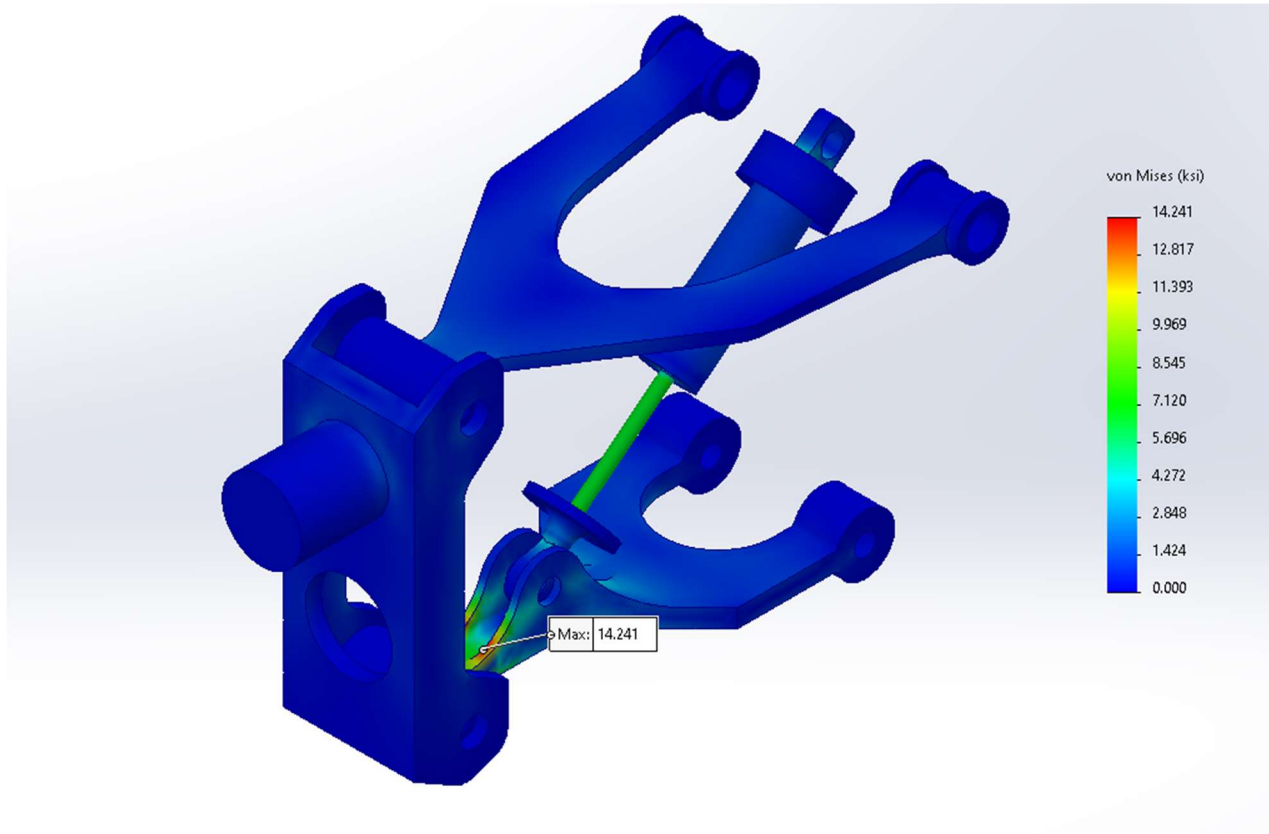


Figure 13 - Max Von Mises - locked shock

The stress in the X direction shows that the top of the lower suspension arm is under the most stress in compression, while the lower side is in tension indicating this area is put under a bending stress. All configurations have similar stress values, around 11.5 and 9 ksi for the compression and tension sections respectively, figures 14 and Appendix D.

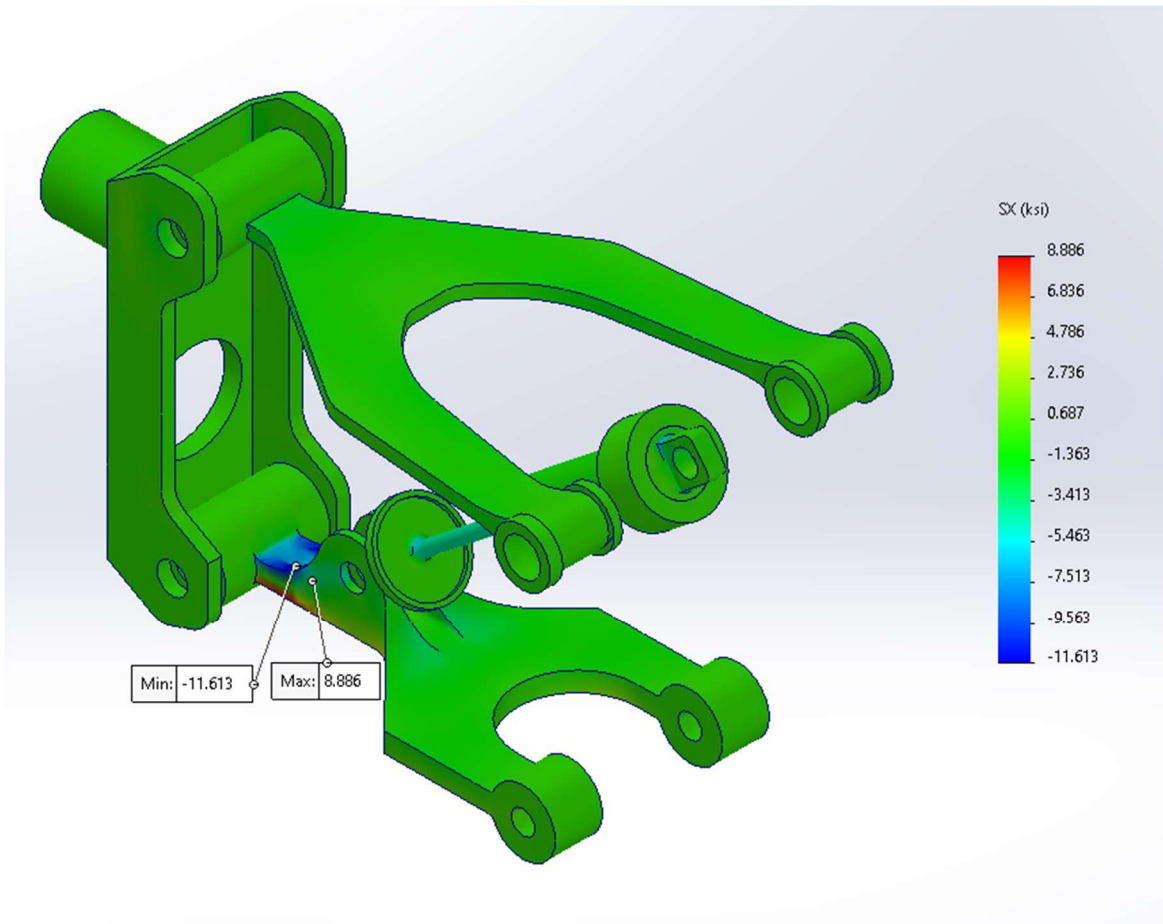


Figure 14 - Max & Min X stress - locked shock

The maximum Y deflection between the different configurations varies by almost half an inch. The maximum occurs with the 450 lb shock where the assembly deflects up by 0.4 inches, figure 15. The 900 lb shock deflects 0.2 inches while the locked-out shock and isolated model have almost no deflection as both can only defect through material deformation, Appendix D.

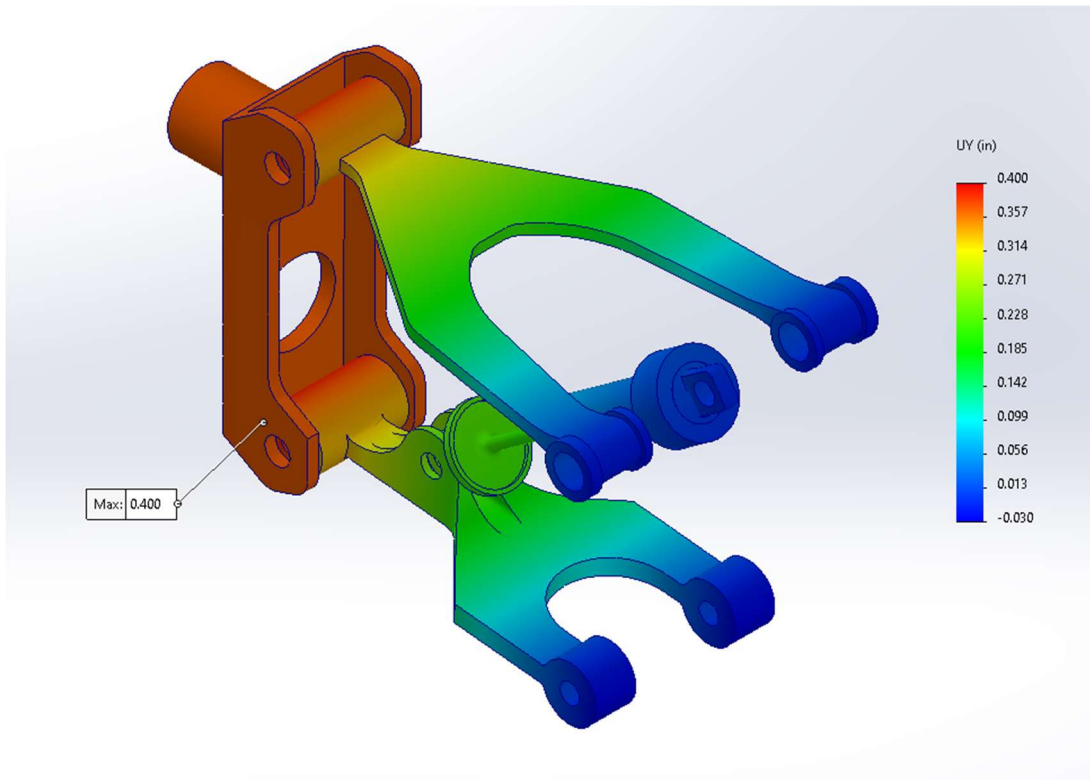


Figure 15 - Y deflection - 450 lb shock

The optimization study found an optimal thickness and base dimensions of 0.1023 and 0.177 inches respectively. This lowered the mass from 0.28 lbs to 0.23 lbs with a minimum factor of safety of 3.7. The new maximum Von Mises stress was 27.9 ksi. Figure 16 shows the factor of safety plot, other relevant plots can be seen in Appendix D.

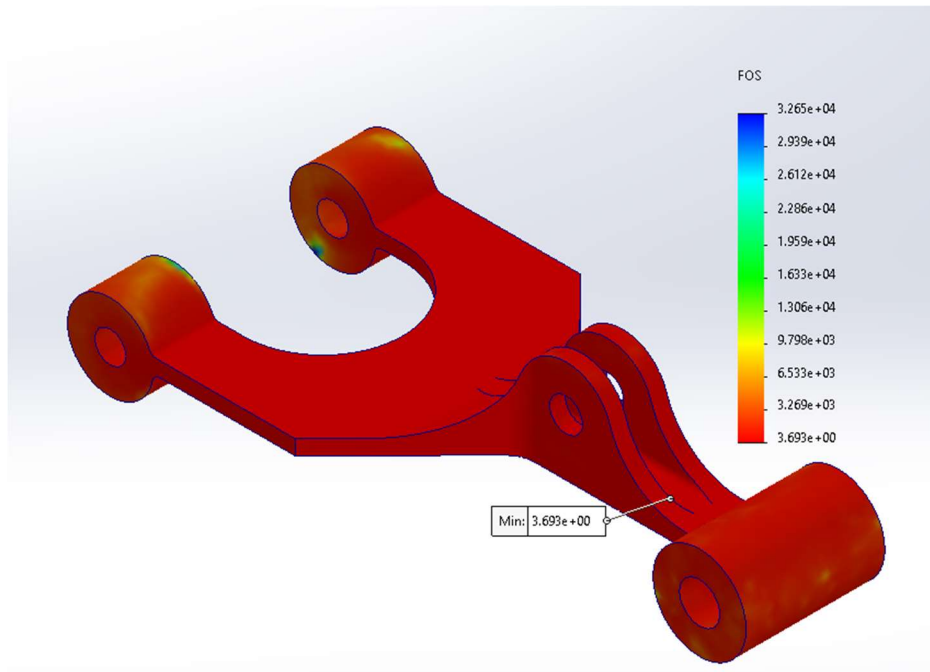


Figure 14 - Von Mises criteria FOS - Optimized arm

Discussion

Within the full assembly the maximum stress remains very similar between the stiff shock and spring shocks. The stress is always the most concentrated around the same part of the lower suspension arm. When the shock is stiff more stress is moved along the shock arm itself. Though the stresses remain similar, the deflection of the system changes with different springs. The locked-out shock system bends 0.003 inches while the 450 lbs spring deflects the most at 0.4 inches. These results indicate that the system can be operated with different shocks to achieve different deflections without changing the stresses on the system. The main limitation of the assembly model is that it does not take into account any stresses or friction within the hinges or pin connections. This model also assumes static forces and does not study potential for fatigue.

Since the stresses remain the same independent from the shock the lower suspension arm being isolated should maintain accurate results. The simulation results are very similar to the results of the whole assembly simulations. With the max stress around the fillet supporting the shock connection. Since this model only uses reaction forces the deflection is not indicative of the whole model. The maximum stress found in the MoM is different by nearly 2 ksi compared to this model. Though these calculations are a decent estimate they don't mimic the FEA perfectly. This difference is because the MoM calculations cannot perfectly take into account the model geometry, or the location of the reaction forces applied.

The optimization study was able to reduce the total mass of the lower suspension arm by 19.2% by decreasing the gap dimension and thickness. This optimization kept the minimum factor of safety above 3.5. The maximum stress remained in the same location. The dimensional changes made in this optimization may require a redesign where the lower suspension arm and the shock plunger connect as the spacing changed.

Conclusion

The goal of this FEA study was to analyze and optimize a wishbone suspension assembly. Specifically, the lower suspension arm where the maximum stress occurs. It was found that the system experienced expected displacement under different shock conditions while maintaining almost identical stresses throughout the remainder of the system.

The optimization of the lower suspension arm was successful managing to reduce the overall mass while keeping the desired factor of safety.

While the optimization was successful there is potential for further optimization. The stress remained concentrated throughout the same area with little stress elsewhere in the part. This indicates that there may be other areas that could be optimized for more weight savings.

A further study of the lower suspension arm in isolation with a focus on redesigns along the high stress areas and mass savings elsewhere in the part would be good next steps. Nonuniform thicknesses are likely a good starting point for these potential improvements.

Appendix A – Material Properties

AISI 4340 Steel

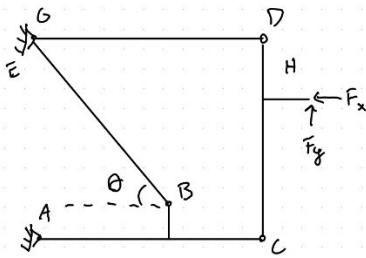
Property	Value	Units
Elastic Modulus	2.97e+7	psi
Poisson's Ratio	0.32	N/A
Shear Modulus	1.16e+7	psi
Mass Density	0.284	lb/in ³
Tensile Strength	1.61e+5	psi
Yield Strength	1.03e+5	psi

Cast Carbon Steel

Property	Value	Units
Elastic Modulus	2.90e+7	psi
Poisson's Ratio	0.32	N/A
Shear Modulus	1.10e+7	psi
Mass Density	0.282	lb/in ³
Tensile Strength	6.999e+4	psi
Yield Strength	3.60e+4	psi

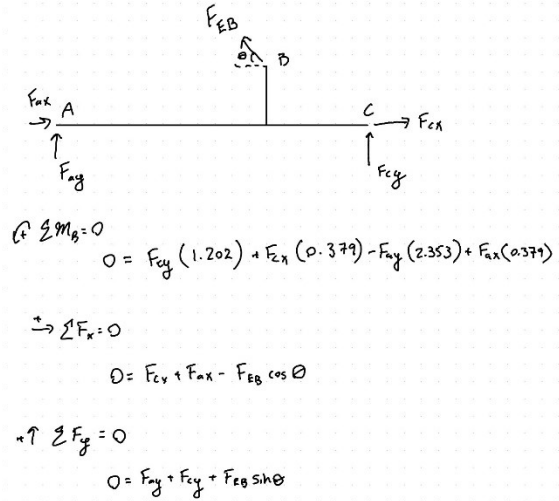
Appendix B – Statics Hand Calculations

Statics of Wishbone
Suspension - Jackson McLeod

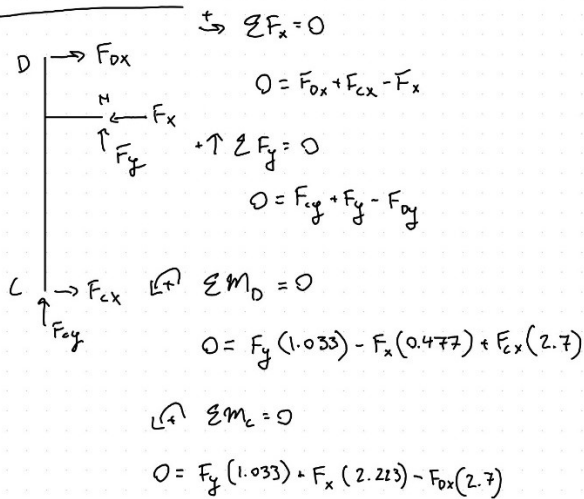


$$\theta = \tan^{-1}\left(\frac{2.321}{2.494}\right) = 39.3465^\circ$$

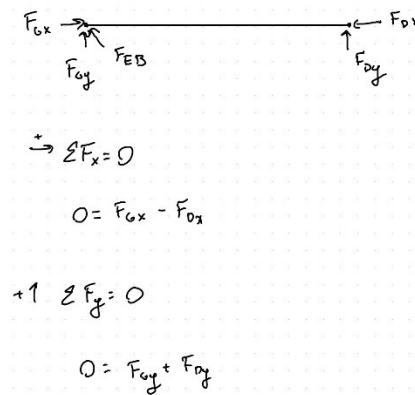
FBD ABC



FBD DHC



FBD - GD



Appendix C – EES MoM Calculations

Globe Definitions

$$F_x = 75 \text{ [lbf]}$$

$$F_y = 40 \text{ [lbf]}$$

$$\theta = 38.35 \text{ [deg]}$$

FBD DHC

$$0 = F_{dy} \text{ Acts like two force member}$$

$$0 = F_{dx} + F_{cx} - F_x \text{ Sum of forces in X}$$

$$0 = F_{cy} + F_y - F_{dy} \text{ Sum of forces in Y}$$

$$0 = F_y \cdot 1.033 \text{ [in]} - F_x \cdot 0.477 \text{ [in]} + F_{cx} \cdot 2.7 \text{ [in]} \text{ Moment about D}$$

FBD ABC

$$0 = F_{cx} + F_{ax} - F_{EB} \cdot \cos(\theta) \text{ Sum of forces in X}$$

$$0 = F_{ay} + F_{cy} + F_{EB} \cdot \sin(\theta) \text{ Sum of forces in Y}$$

$$0 = F_{cy} \cdot 1.202 + F_{cx} \cdot 0.379 \text{ [in]} - F_{ay} \cdot 2.353 \text{ [in]} + F_{ax} \cdot 0.379 \text{ [in]} \text{ Moment about B}$$

FBD GD

$$0 = F_{gx} + F_{dx} \text{ Sum of forces in X}$$

$$0 = F_{gy} + F_{dy} \text{ Sum of forces in Y}$$

Verification of Max X Stress

$$A_c = 0.07827301 \text{ [in}^2\text{]}$$

$$I = 0.00028399 \text{ [in}^4\text{]}$$

$$y = 0.1283 \text{ [in]}$$

Axial Stress

$$F_{xtot} = F_{cx}$$

$$\sigma_{x,axial} = \frac{F_{xtot}}{A_c}$$

Bending Stress

$$M_{bending} = F_{EB} \cdot \cos(\theta) \cdot 0.29 - F_{EB} \cdot \sin(\theta) \cdot 0.45 - F_{cy} \cdot 0.7 + F_{cx} \cdot 0.09$$

$$\sigma_{bend} = \frac{M_{bending} \cdot y}{I}$$

Total Stress

$$\sigma_x = \sigma_{bend} + \sigma_{x,axial}$$

$A_c = 0.07827 \text{ [in}^2\text{]}$	$F_{ax} = 65.52$	$F_{ay} = -10.21$	$F_{cx} = -2.054$
$F_{cy} = -40$	$F_{dx} = 77.05$	$F_{dy} = 0$	$F_{EB} = 80.93$
$F_{gx} = -77.05$	$F_{gy} = 0$	$F_x = 75 \text{ [lbf]}$	$F_{xtot} = -2.054$
$F_y = 40 \text{ [lbf]}$	$I = 0.000284 \text{ [in}^4\text{]}$	$M_{bending} = 23.63$	$\sigma_{bend} = 10674$
$\sigma_x = 10648$	$\sigma_{x,axial} = -26.24$	$\theta = 38.35 \text{ [deg]}$	$y = 0.1283 \text{ [in]}$

Appendix D – FEA Result Plots

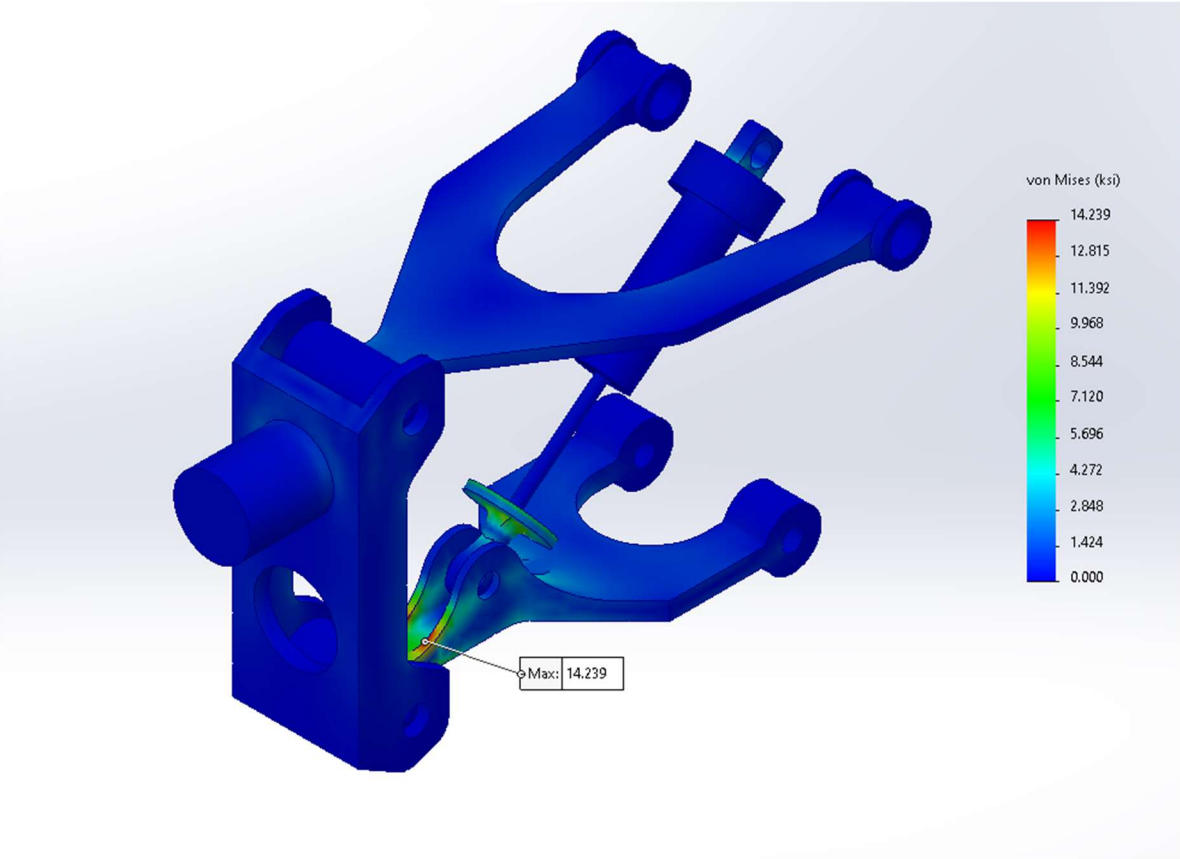


Figure D1 - Max Von Mises - 450 lb shock

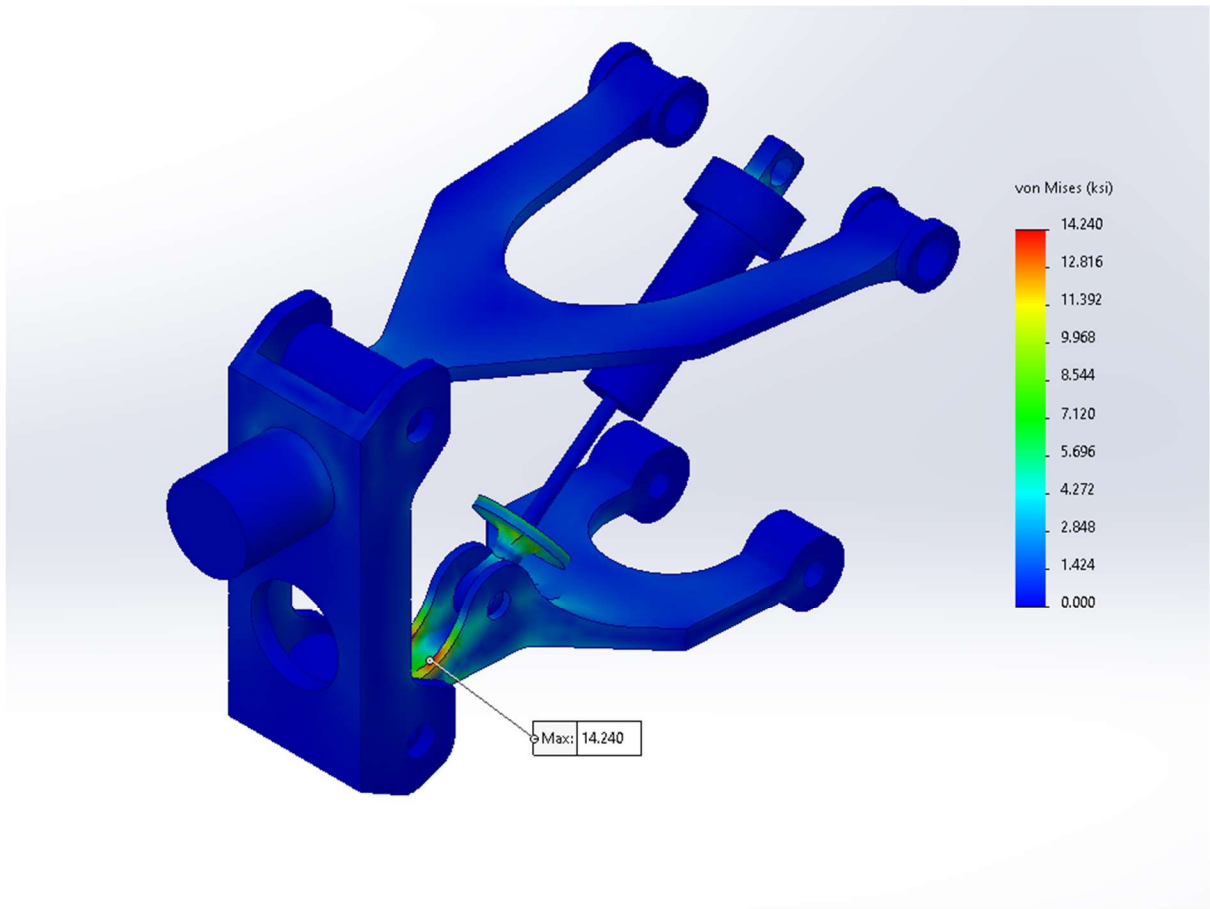


Figure D2 - Max Von Mises - 900 lb shock

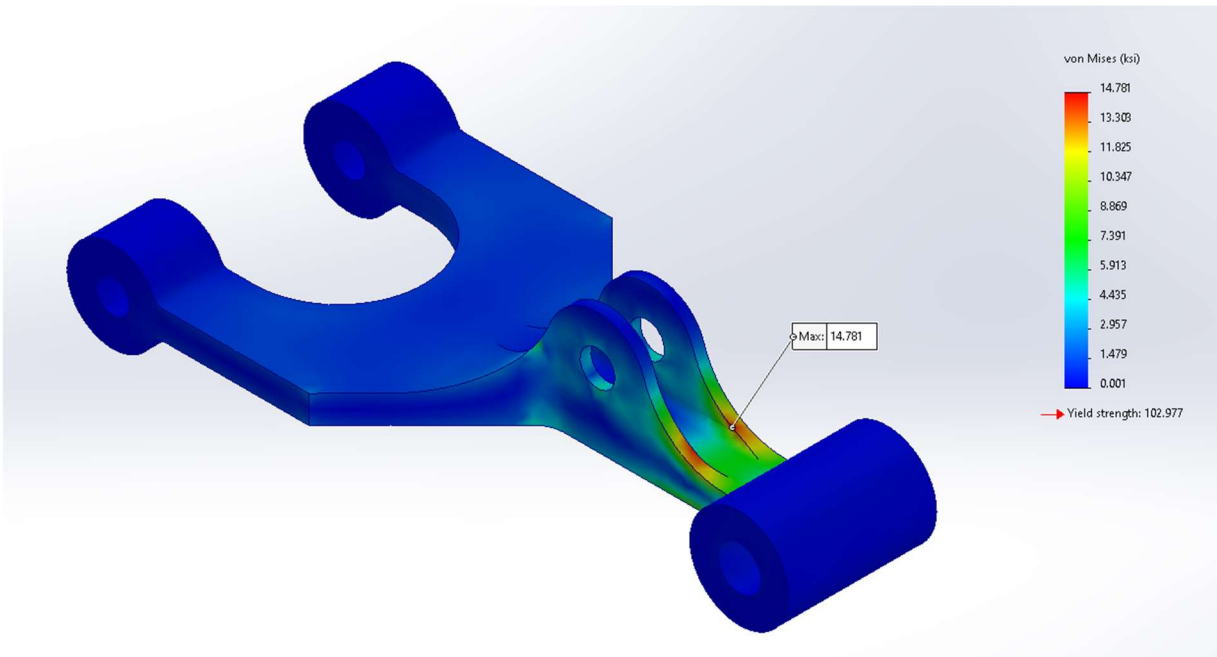


Figure D3 - Max Von Mises - Isolated lower suspension arm

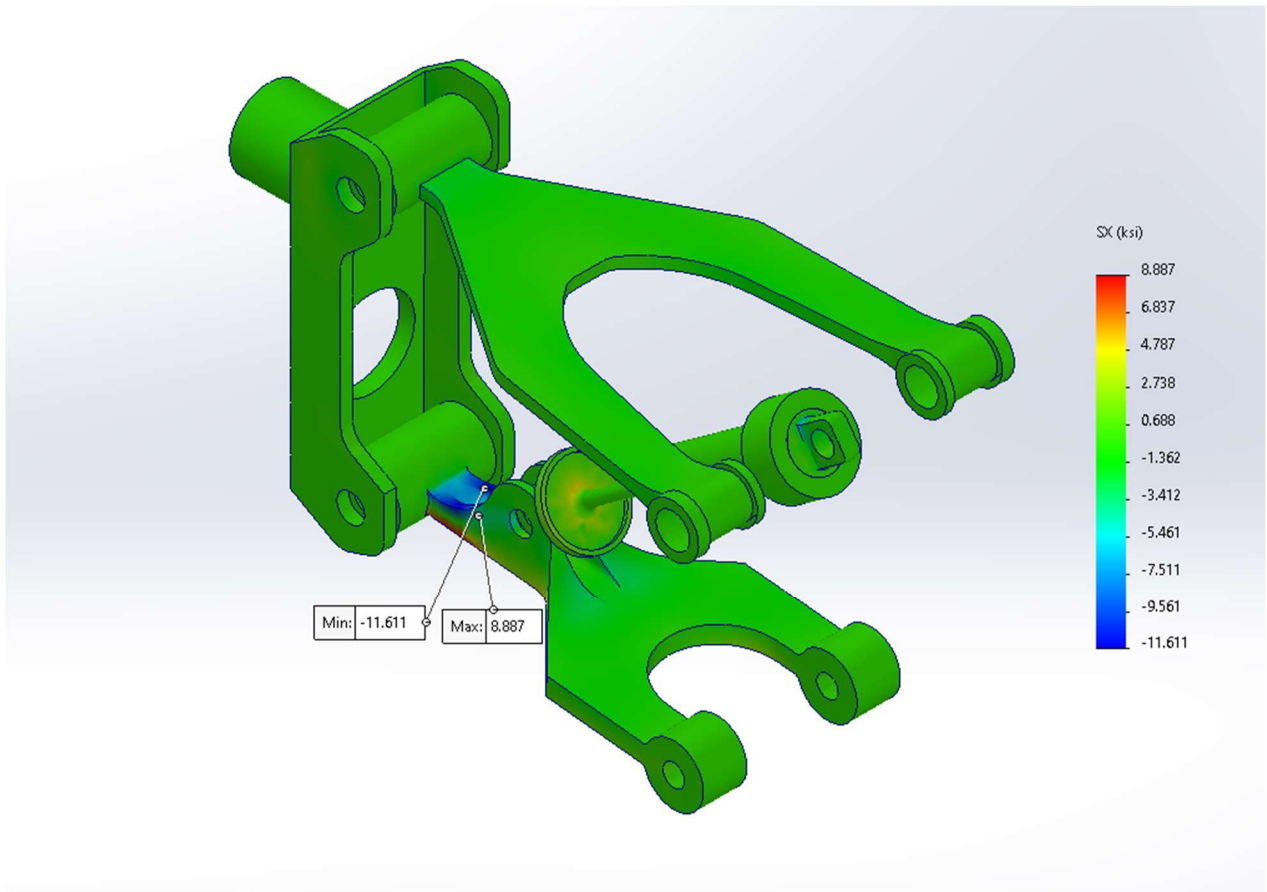


Figure D4 - Max & Min X stress - 450 lb shock

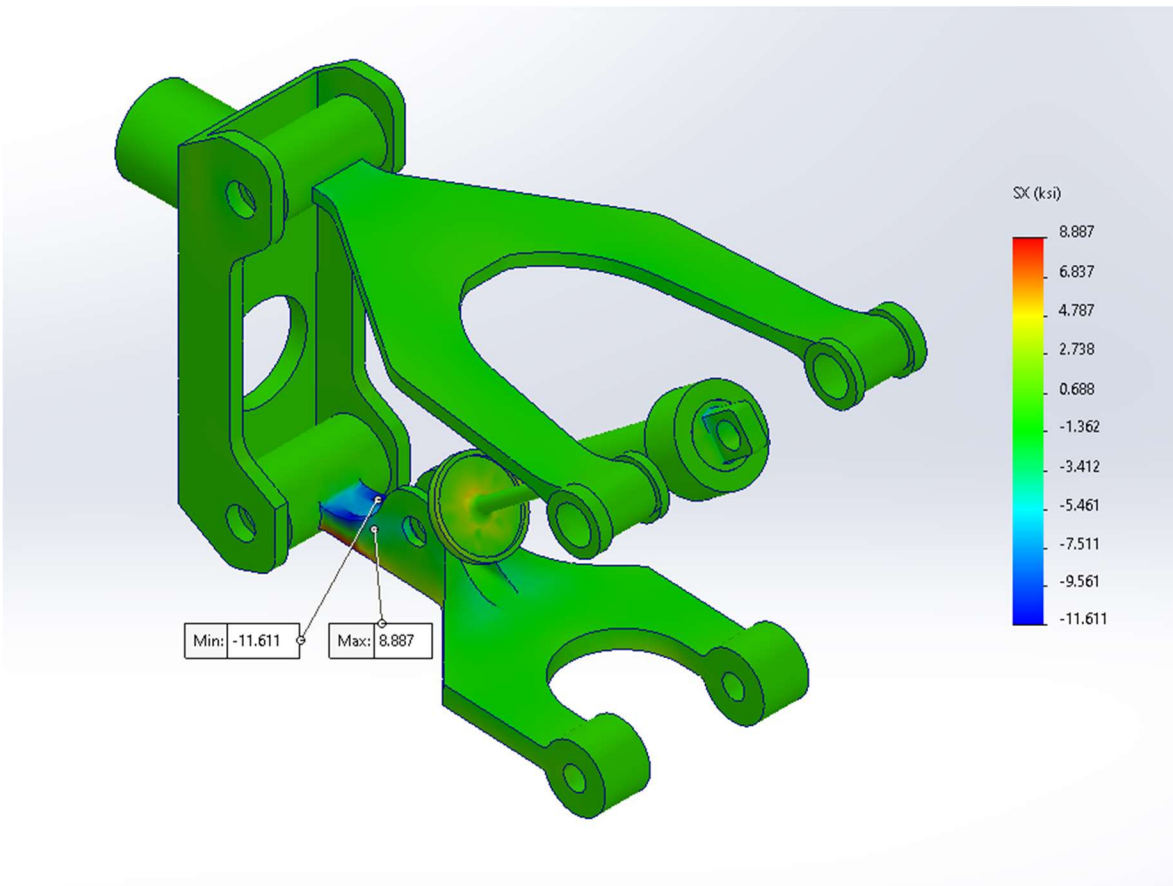


Figure D5 - Max & Min X stress - 900 lb shock

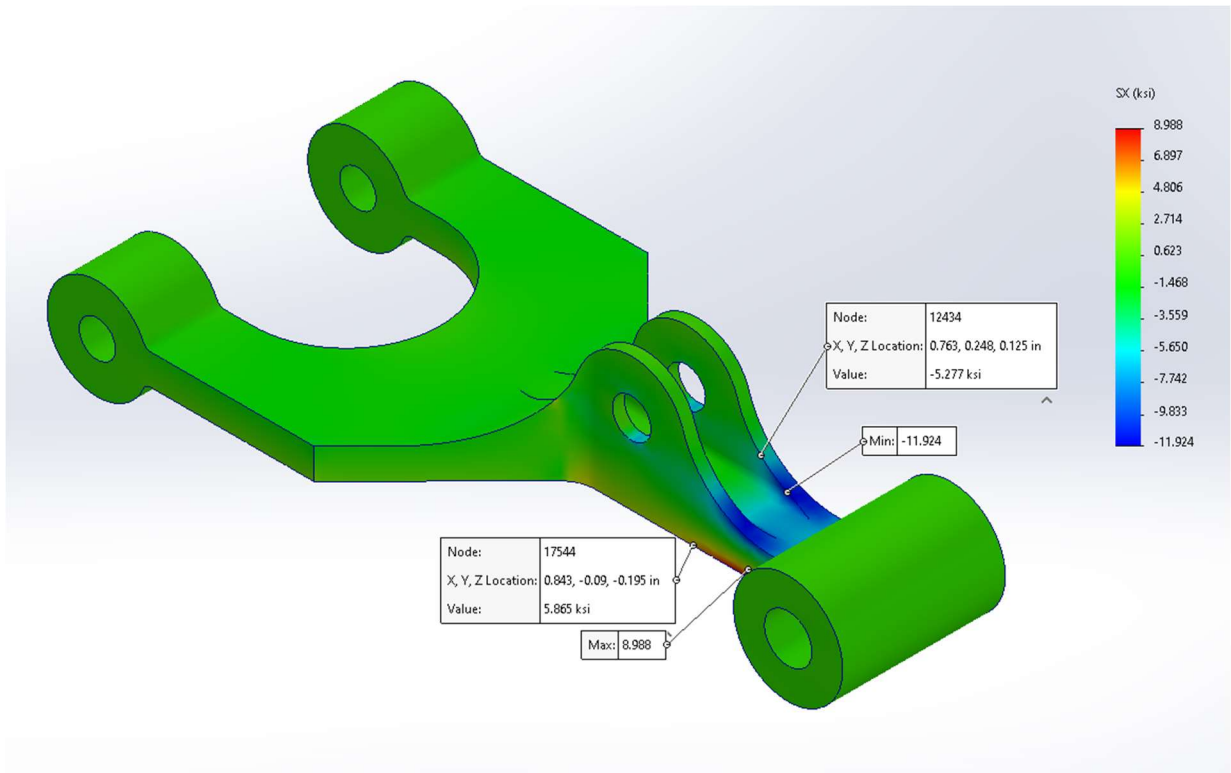


Figure D6 - Max & Min X stress - Isolated lower suspension arm

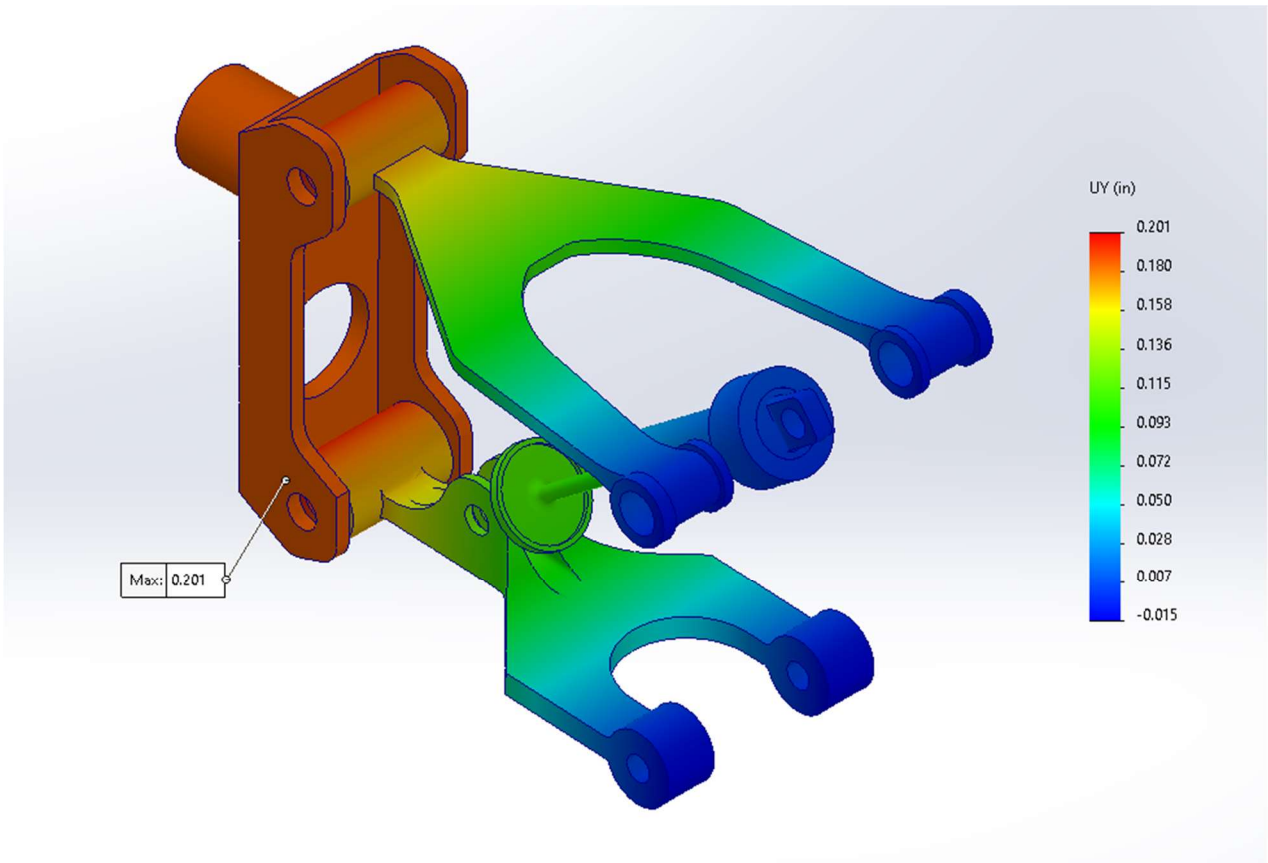


Figure D7 - Y deflection - 900 lb shock

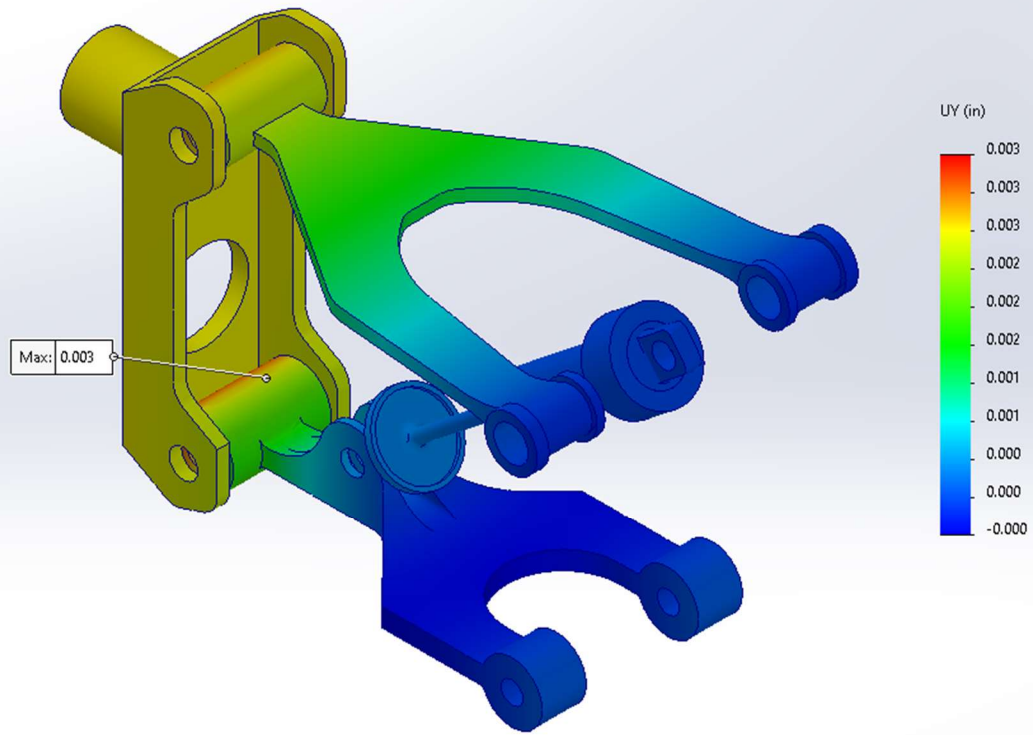


Figure D8 - Y deflection - locked shock

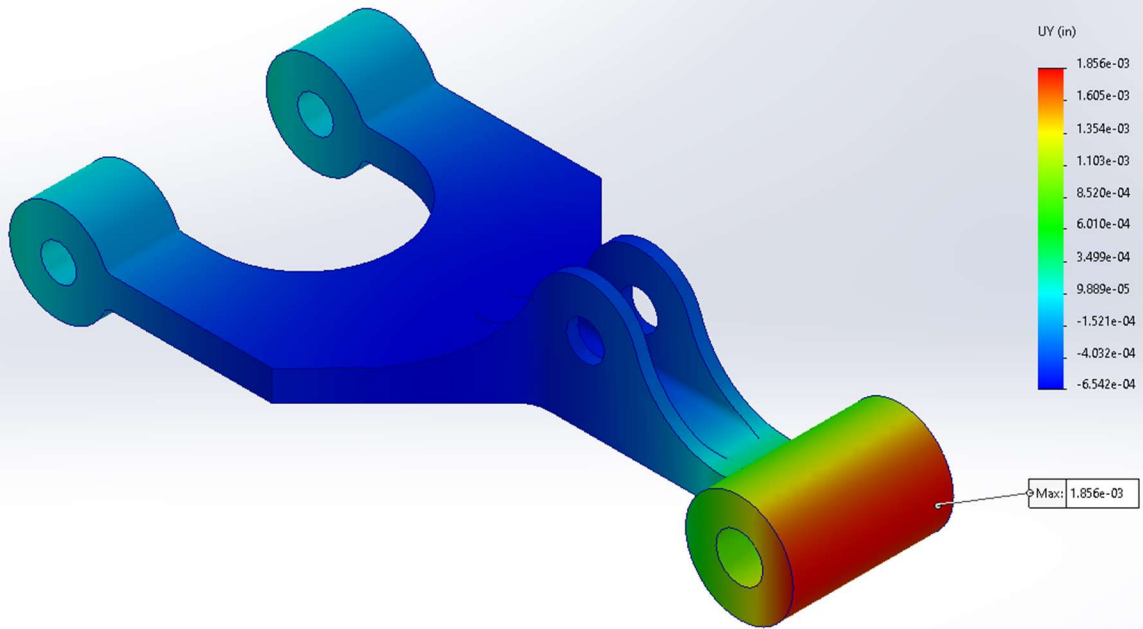


Figure D9 - Y deflection - isolated lower suspension arm

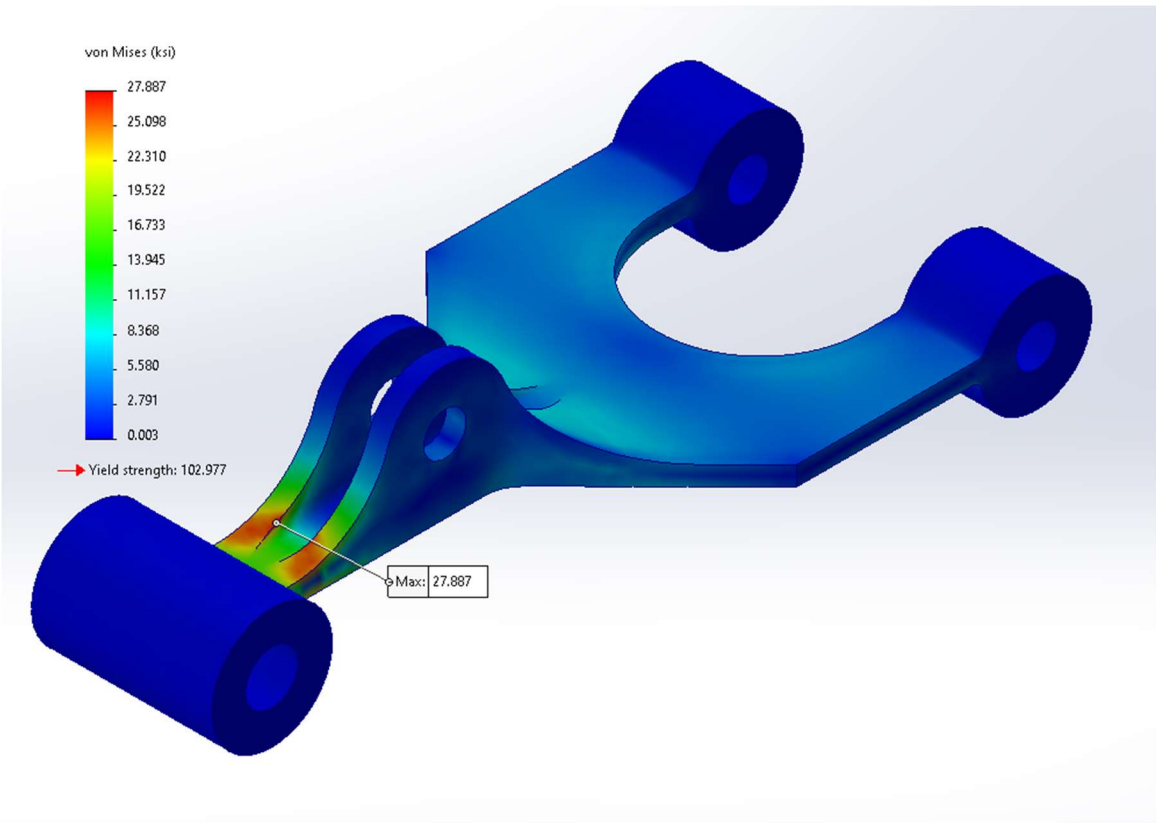


Figure D10 - Max Von Mises - Optimized arm

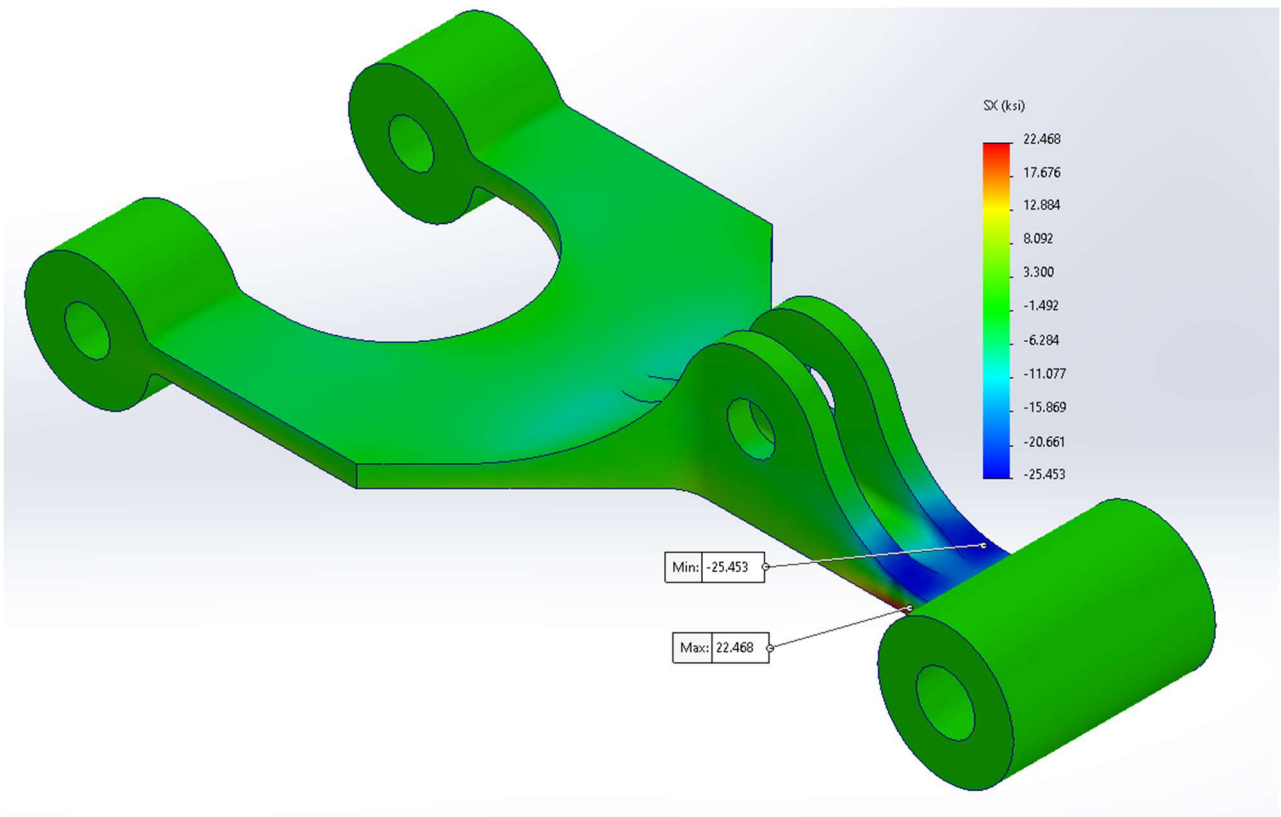


Figure D11 - Min & Max X stress - Optimized arm